Absorption spectrum of atomic impurities in isotopic mixtures of liquid helium

David Mateo, Alberto Hernando, Manuel Barranco, Ricardo Mayol, and Martí Pi
Departament ECM, Facultat de Física, and IN²UB, Universitat de Barcelona, Diagonal 647, 08028 Barcelona, Spain
(Received 7 February 2011; published 6 May 2011)

We theoretically describe the absorption spectrum of atomic impurities in isotopic mixtures of liquid helium within a zero-temperature density functional approach. Two situations are considered. In the first one, the absorption spectrum of Na atoms attached to $^4He_{1000}$-$^3He_{N_3}$ droplets with N_3 values from 100 to 3000 is presented as a case study of an impurity that does not dissolve into helium droplets. In the second one, the absorption spectrum of Mg atoms in liquid ^{3}He-^{4}He mixtures is presented as a case study of an impurity dissolved into liquid helium. We have found that the absorption spectrum of the impurity is rather insensitive to the isotopic composition because the line shift is mostly affected by the total He density around the impurity, not by its actual composition. For bulk liquid mixtures, results are presented as a function of pressure at selected values of the ^{3}He concentration. The results for isotopically pure ^{3}He and ^{4}He liquids doped with Mg are compared with available experimental data.

DOI: 10.1103/PhysRevB.83.174505 PACS number(s): 67.60.−g, 78.40.−q, 32.30.Jc

I. INTRODUCTION

The study of the absorption spectrum of impurities in liquid helium and its droplets has drawn considerable interest because it is a powerful tool to investigate the structure of the dopant-liquid complex, having become a classical field in optical spectroscopy. The optical properties of impurities in liquid ^{4}He and its droplets have been reviewed in Refs. 1 and 2, respectively.

Electronic spectroscopy studies have been carried out for atomic impurities in ^{4}He, and to a lesser extent, in ^{3}He.[3–5] Only very recently, the electronic absorption spectrum of an atomic impurity—a Ca atom—in mixed ^{3}He-^{4}He droplets has been reported and analyzed within density functional (DF) theory.[6] A distinct feature of Ca atoms in mixed helium droplets is that, depending on the size and isotopic composition of the droplet, it may reside at the ^{3}He-^{4}He interface. Therefore, one would expect that its electronic spectrum might shed light on the structure of that interface, as this spectrum is affected by the liquid environment around the impurity.

Experiments on doped mixed droplets have to face the serious problem of determining the actual composition of the system. This is not easy because of the large number of atoms, mostly of ^{3}He, that are evaporated off the droplet after the dopant pick-up, altering the initial composition of the droplet in a way that is difficult to ascertain. The initial composition is not easy to determine either. In contrast, experiments in liquid mixtures may be carried out under well-controlled conditions, fixing, e.g., the ^{3}He concentration $x_3 = N_3/(N_3 + N_4)$ and particle density $\rho = (N_3 + N_4)/V$ and temperature (T) of the mixture, which in turn determine the total pressure (P) throughout the equation of state of the fluid.

In this work, we aim to study the effect of isotopic composition on the absorption spectrum of atomic impurities in both finite (droplets) and extensive (liquid) helium systems. We present results for the $3p \leftarrow 3s$ transition of Na attached to ^{3}He-^{4}He droplets, complementing those we have previously published for Ca.[6] It is well known experimentally[7] and theoretically[8] that, because of the limited solubility of ^{3}He in ^{4}He at low temperatures,[9] mixed droplets have a core-shell structure made of nearly pure ^{4}He and ^{3}He, respectively. Since Na atoms do not dissolve into helium droplets, the *a priori* most interesting situation is when the number of ^{3}He atoms, N_3, is rather small as compared to that of ^{4}He, N_4. Otherwise, the environment around Na is made of pure ^{3}He and one should not expect any difference with the absorption spectrum of Na in isotopically pure ^{3}He droplets.[3]

At variance with the droplet situation, ^{3}He segregation in liquid helium mixtures at low temperatures only appears for concentrations above a critical value that depends on pressure.[9] Hence, it is plausible that the absorption spectrum could be sensitive to the x_3 value of the mixture. To check this hypothesis, we present calculations of the absorption spectrum around the $3s\,3p\ ^1P_1 \leftarrow 3s^2\ ^1S_0$ transition of Mg atoms in liquid helium mixtures for selected values of x_3 and P.

This work is organized as follows. In Sec. II, we briefly recall the DF method used to obtain the structure of doped helium mixtures, drops, and bulk liquid as well, and the procedure used to determine the absorption spectrum incorporating shape fluctuations of the liquid bubble around the dopant. The absorption spectrum of Na in $^4He_{1000}$-$^3He_{N_3}$ droplets with $N_3 = 100$ to 3000, and that of Mg in ^{3}He-^{4}He liquid mixtures for selected values of x_3 and P, is discussed in Sec. III. Finally, a summary is presented in Sec. IV.

II. METHOD

A. Density functional description of the ground state of doped isotopic mixtures

The energy of the Na-droplet complex is written as a functional of the Na wave function $\Phi(\mathbf{r})$, the ^{4}He effective macroscopic wave function $\Psi(\mathbf{r}) = \sqrt{\rho_4(\mathbf{r})}$, where $\rho_4(\mathbf{r})$ is the ^{4}He atomic density normalized to N_4 atoms, and the ^{3}He particle and kinetic energy densities $\rho_3(\mathbf{r})$ (normalized to N_3 atoms) and $\tau_3(\mathbf{r})$.[10] We have used a Thomas-Fermi

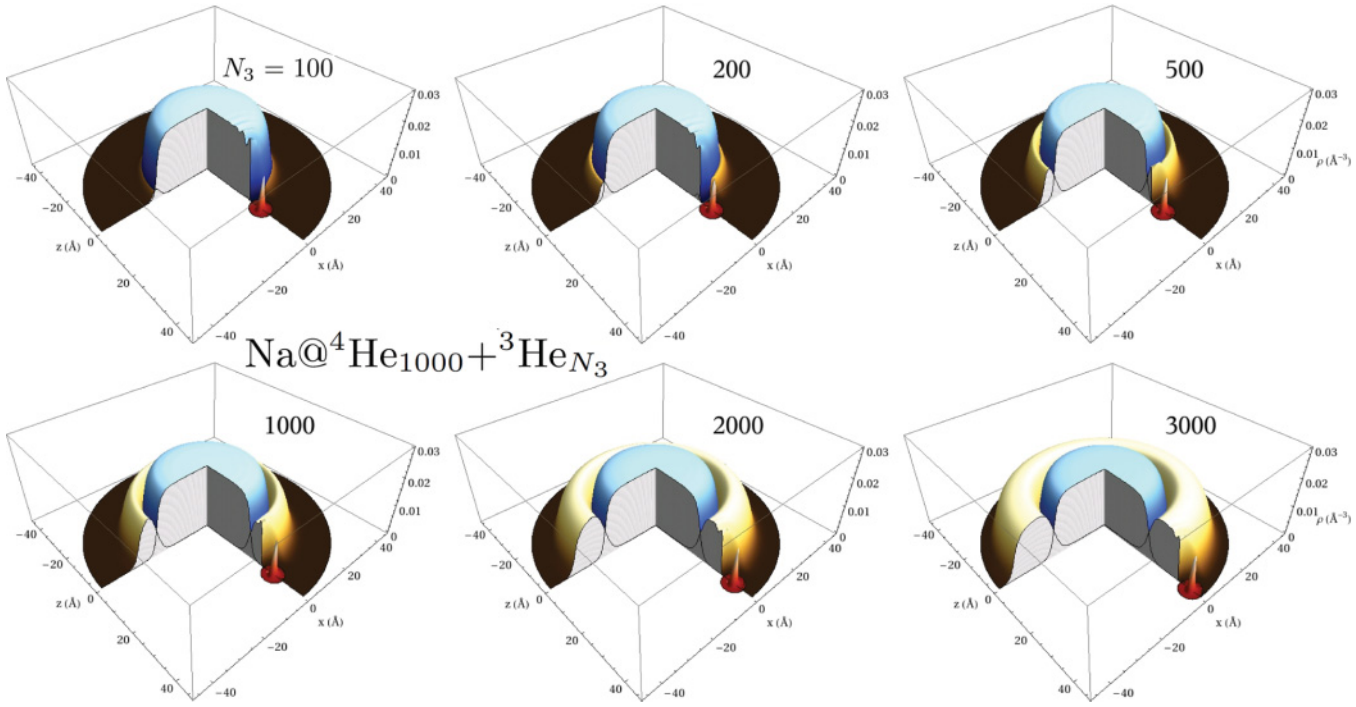

FIG. 1. (Color online) Three-dimensional view of $\mathrm{Na@^4He_{1000}+^3He_{N_3}}$ droplets for different N_3 values. Also shown is the probability density of Na in arbitrary units.

approximation to write $\tau_3(\mathbf{r})$ as a function of $\rho_3(\mathbf{r})$ and its gradient.[3] Within the pair potential approximation, we have[11]

$$E[\Psi,\Phi,\rho_3,\tau_3] = \frac{\hbar^2}{2\,m_{^4\mathrm{He}}}\int d\mathbf{r}\,|\nabla\Psi(\mathbf{r})|^2 + \int d\mathbf{r}\,\mathcal{E}(\rho_4,\rho_3,\tau_3) + \frac{\hbar^2}{2\,m_{\mathrm{Na}}}\int d\mathbf{r}\,|\nabla\Phi(\mathbf{r})|^2 + \iint d\mathbf{r}\,d\mathbf{r}'\,|\Phi(\mathbf{r})|^2\,V_{X^2\Sigma}(|\mathbf{r}-\mathbf{r}'|)\,\rho_{3+4}(\mathbf{r}'). \quad (1)$$

The Na-He $X\,^2\Sigma$ pair potential has been taken from Ref. 12. The equations resulting from the variations of Eq. (1) with respect to Ψ, Φ, and $\rho_3(\mathbf{r})$ are self-consistently solved as indicated in Ref. 11.

Figure 1 displays a three-dimensional view of $\mathrm{Na@^4He_{1000}}+^3\mathrm{He}_{N_3}$ droplets for several N_3 values, and the probability density of Na, $|\Phi(\mathbf{r})|^2$, in arbitrary units. The figure shows the above-mentioned core-shell distribution of ^{4}He and ^{3}He atoms in the droplet, as well as the known result that Na does not dissolve into them. In this respect, it is illustrative to compare the results for Na with those for Ca (see Fig. 2 of Ref. 6 corresponding to $\mathrm{Ca@^4He_{1000}}+^3\mathrm{He}_{2000}$). So far, Ca is the only known impurity that is dissolved into ^{4}He but not into ^{3}He droplets, and for this reason it may sink into the fermionic component until reaching the surface of the bosonic core. More attractive impurities like OCS reside in the bulk of the core, thus they are instrumental in the discussion of superfluidity at the nanoscale.[7] Here we discuss the remaining case of an impurity that resides at the surface of the droplet irrespective of the isotope. One of the cuts in Fig. 1 displays the pure ^{3}He-^{4}He interface showing the building up of the ^{3}He shell as N_3 increases. It is worth noting that, with a core of 1000 ^{4}He atoms, a large amount of ^{3}He ($N_3 \sim 2000$) is needed before the density of the fermionic shell reaches that of liquid ^{3}He at saturation; see also Ref. 8. The other cut displays the doped ^{3}He-^{4}He interface. Notice that for the $N_4 = 1000$ droplet, one should not expect that the absorption spectrum of Na onto $\mathrm{^4He_{1000}}+^3\mathrm{He}_{N_3}$ differs much from that of Na onto an isotopically pure ^{3}He droplet of similar size if $N_3 \gtrsim 1000$.

The starting point for describing a Mg atom in liquid helium mixtures is also Eq. (1). The Mg-He $X\,^1\Sigma$ pair potential has been taken from Ref. 13. In this case, instead of fixing the number of atoms N_3 and N_4, the asymptotic ρ_3 and ρ_4 densities far from the impurity have been fixed to those of the undoped mixture. In practice, we work at fixed P and x_3 values, which in turn fix the ρ_3 and ρ_4 values (and the corresponding chemical potentials) through the $T = 0$ equation of state supplied by our DF.[10] Details of the procedure and method used for solving the variational equations can be found in Ref. 14 for an electron bubble in liquid ^{4}He. The generalization to helium mixtures and atomic impurities is straightforward.

We want to emphasize that our method yields a self-consistent and accurate description of the thermodynamics of undoped liquid mixtures at zero temperature, a necessary starting point to address the properties of the doped system. In particular, it reproduces the $T = 0$ phase diagram of the mixture. Figure 2 shows the calculated phase diagram obtained as explained in Ref. 15.

The top and bottom panels of Fig. 3 show the helium density profile around Mg in the case of isotopically pure ^{4}He and ^{3}He liquids for three different pressures. It can be seen that the helium density is strongly modulated around the impurity, slowly evolving toward the bulk liquid density as the distance

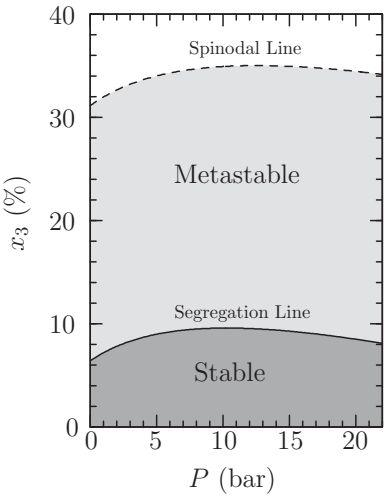

FIG. 2. Calculated phase diagram of the ^{4}He-^{3}He liquid mixture at $T = 0$. The solid line between stable and metastable regions is the maximum solubility line of ^{3}He into ^{4}He, and the dashed line is the spinodal line.

from the impurity increases. Notice also how the liquid density increases as P does, and how the radius of the bubble around the impurity is slightly larger for ^{3}He than for ^{4}He because of the surface tension being smaller for ^{3}He than for ^{4}He. This figure shows that, even for rather weakly interacting dopants such as Mg, the actual structure of the liquid cannot be easily guessed or represented by simple parametrizations. This is especially so in the case of isotopic liquid mixtures; see the middle panel of Fig. 3.

These density profiles already give a first idea of what to expect from the study of the absorption peak as a function of P: the shift increases as the density does, and therefore it will also increase with P. Similarly, the shift should be larger for Mg in isotopically pure ^{4}He than in isotopically pure ^{3}He at given P, as the He-Mg interaction is the same irrespective of the isotope. These facts have been established experimentally.[4,5]

The middle panel of Fig. 3 shows the density profile at $P = 10$ bar for $x_3 = 9\%$. It can be seen from Fig. 2 that these conditions allow us to carry out the calculation for nearly the largest possible ^{3}He concentration before segregation. For the sake of comparison, the result for pure ^{4}He is also shown. Whereas the results displayed in the other panels of Fig. 3 are known to some extent, to the best of our knowledge the density profiles of isotopic mixtures of liquid helium around an attractive impurity have not been previously determined. Along the lines of the other two panels, one would expect a very weak dependence of the atomic shift on the composition of the mixture. Comparing the total helium densities displayed in the middle panel of Fig. 3, the atomic shift might be slightly larger for liquid ^{4}He than for the mixture at the same pressure. In the next section, we address these issues in detail, confirming these expectations.

We would like to close the discussion of the density profiles by pointing out two interesting characteristics of the liquid mixture at low temperatures, relevant for the forthcoming discussion of the absorption spectrum. The first feature is that, as can be seen from Fig. 3, substituting ^{4}He by ^{3}He atoms at a given P does not result in a sizable change in the liquid

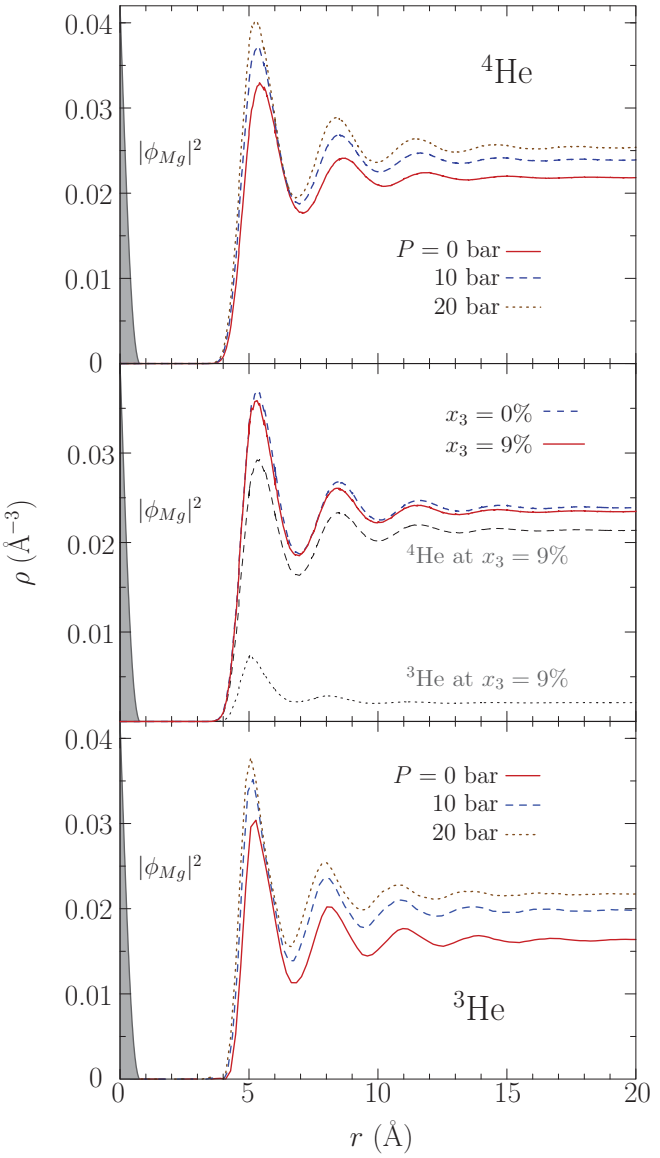

FIG. 3. (Color online) Selected density profiles of the liquid helium mixture around an Mg impurity whose probability density in represented in arbitrary units. Top panel: pure ^{4}He. Bottom panel: pure ^{3}He. Middle panel: density profiles at $P = 10$ bar for $x_3 = 9\%$. Solid line, total density; thin dashed line, ^{4}He density; dotted line, ^{3}He density. For the sake of comparison, the profile of isotopically pure ^{4}He is also shown (dashed line).

total density. This is due to the high incompressibility of liquid helium. The other feature worth noting is that ^{3}He atoms do not segregate around the impurity coating the surface of the bubble. This is due to the large zero-point energy that a ^{3}He atom would have in such a small cavity, and it is more marked the larger the impurity-helium interaction is. As a consequence, the impurity bubble is coated by ^{4}He atoms and not by ^{3}He, in spite of the density increase of both isotopes at the first solvation shell, allowing the appearance of the rovibrational spectrum of OCS molecules in helium droplets[7] that otherwise would be quenched by the presence of normal-phase ^{3}He atoms. This is at variance with the situation at the free surface of a mixed drop or liquid mixture, where the existence of Andreev states

bearing a large capacity of hosting ^{3}He atoms makes possible the accumulation of this isotope at the surface.[8]

B. Absorption spectrum

To determine the absorption spectrum of an impurity atom embedded in a condensed system, it is customary to use Lax's method,[16] together with the diatomics-in-molecules approach.[17] This is basically the method we have followed,[11] once the ground state (gs) of the dopant-helium mixture (droplet or bulk liquid) has been determined. The $^2\Pi$ and $^2\Sigma$ excited pair potentials for Na-He are from Ref. 18, and the $^1\Pi$ and $^1\Sigma$ ones for Mg-He are from Ref. 19. In the case of Na, we have also considered the spin-orbit splitting.[11]

With only these ingredients, the model yields a good description of the absorption energies—provided the pair potentials are accurate enough—but the shape, especially the width, of the absorption line is poorly reproduced. The well-known reason for this drawback is the neglect of the coupling of the impurity dipole excitation to the shape fluctuations (modes) of the liquid cavity around it. Including this coupling in the calculation yields a much better agreement with experiments. This is illustrated, e.g., in Ref. 20 for Mg atoms in ^{4}He droplets and in Ref. 21 for electron bubbles in liquid ^{4}He. Taking into account shape fluctuations is very cumbersome if the impurity bubble is not spherical. The situation is far more complex for liquid ^{3}He and mixtures because the modes of the cavity are difficult to determine.

Shape fluctuations are effortlessly calculated in quantum Monte Carlo simulations of the absorption spectrum[22–24] by taking advantage of the information carried out by the quantum "walkers." Somewhat inspired by this atomiclike simulation, an easy-to-implement method has been proposed within DF theory to include shape fluctuations, and it has been applied to the case of Cs in liquid ^{4}He,[25] and was later adapted to the droplet geometry.[26,27] The extension to the case of isotopic mixtures is straightforward, but for the sake of completeness we present it here as applied to the case of a Na impurity, outlining the method we have followed to determine the absorption spectrum of an impurity in liquid helium.

The Born-Oppenheimer approximation allows the factorization of the electronic and nuclear wave functions, and the Franck-Condon approximation allows the positions of the atomic nuclei to remain frozen during the electronic transition. Within these approximations, the line shape for an electronic transition from the gs to an excited state (ex) is obtained as the Fourier transform of the time-correlation function,

$$I(\omega) \propto \sum_m \int dt e^{-i(\omega+\omega^{\rm gs})t} \int d^3\mathbf{r}\Phi^{\rm gs*} e^{(it/\hbar)H_m^{\rm ex}} \Phi^{\rm gs} , \quad (2)$$

where $\hbar\omega^{\rm gs}$ and $\Phi^{\rm gs}(\mathbf{r})$ are the eigenenergy and eigenfunction of Na in its gs, respectively. The Hamiltonian is $H_m^{\rm ex} = T_{\rm kin} + V_m^{\rm ex}(\mathbf{r})$, where $T_{\rm kin}$ is the kinetic energy operator and $V_m^{\rm ex}(\mathbf{r})$ is the potential energy surface defined by the mth eigenvalue of the excited potential matrix $V(\mathbf{r}) = U(\mathbf{r}) + V_{\rm SO}$, where $U(\mathbf{r})$ is the convolution of the excited pair potentials $^2\Pi$ and $^2\Sigma$ with the *total* helium density $\rho(\mathbf{r})$, as the ^{3}He- and ^{4}He-impurity pair potentials are the same, and $V_{\rm SO}$ accounts for the spin-orbit coupling.[11] Introducing $\Phi^{\rm gs}(\mathbf{r}) = \sum_\nu a_\nu^m \Phi_\nu^m(\mathbf{r})$ in Eq. (2), where $\Phi_\nu^m(\mathbf{r})$ are the eigenfunctions of $H_m^{\rm ex}$ and $a_\nu^m = \int d^3\mathbf{r}\, \Phi_\nu^m(\mathbf{r})^* \Phi^{\rm gs}(\mathbf{r})$ are the Franck-Condon factors, we obtain

$$\begin{aligned} I(\omega) &\propto \sum_m \int dt e^{-i(\omega+\omega^{\rm gs})t} \sum_\nu \left|a_\nu^m\right|^2 e^{i\omega_\nu^m t} \\ &= \sum_m \sum_\nu \left|a_\nu^m\right|^2 \delta\left(\omega + \omega^{\rm gs} - \omega_\nu^m\right) , \end{aligned} \quad (3)$$

where $\hbar\omega_\nu^m$ are the eigenvalues of $H_m^{\rm ex}$.

If the Franck-Condon factors arise from the overlap between the gs and excited states with large quantum numbers, corresponding to the continuous or quasicontinuous spectrum of $H_m^{\rm ex}$, we can assume that $\langle T_{\rm kin}\rangle \ll \langle V_m^{\rm ex}\rangle$, and the Hamiltonian is approximated by $H_m^{\rm ex} \sim V_m^{\rm ex}(\mathbf{r})$. Introducing this approximation in Eq. (2) and integrating over time, we get the semiclassical expression for $I(\omega)$,

$$I(\omega) \propto \sum_m \int d^3\mathbf{r} |\Phi^{\rm gs}(\mathbf{r})|^2 \delta(\omega - [V_m^{\rm ex}(\mathbf{r})/\hbar - \omega^{\rm gs}]) . \quad (4)$$

We have evaluated this expression as follows. First, the helium distribution is stochastically represented by a large number of configurations n_c, of the order of 10^6. Each configuration consists of a set of N positions for the He atoms in the sampling box and one for the impurity. These positions are randomly generated by importance sampling techniques, using the DF helium density $\rho(\mathbf{r})/N$ as the probability density distribution, plus a hard-sphere repulsion between He atoms to approximately take into account He-He correlations. The diameter of the sphere has to be of the order of $h = 2.18$ Å to be consistent with the DF description of the liquid, as h is the length used in the functional to screen the Lennard-Jones interaction between particles and to compute the coarse-grained density.[10] We have chosen a density-dependent sphere radius of the form

$$R_i = R(\mathbf{r}_i) = \frac{h}{2}\left(\frac{\rho_0}{\bar\rho(\mathbf{r}_i)}\right)^{1/3} , \quad (5)$$

where ρ_0 is the saturation density value and $\bar\rho$ is the coarse-grained density, defined as the averaged density over a sphere of radius h. Although this scaling has no effect in the bulk, it is fundamental to correctly reproducing the density in the droplet surface region. The rationale for choosing this R_i is sketched in the Appendix. Lastly, the position of the impurity is also randomly generated using $|\Phi^{\rm gs}(\mathbf{r})|^2$ as the probability density distribution.

To determine the line shape, we obtain for each configuration $\{j\}$ the $V_m^{\rm ex}\{j\}$ eigenvalues of the excited-state energy matrix $\sum_i U(|\mathbf{r}_i^{\{j\}} - \mathbf{r}_{\rm Na}^{\{j\}}|) + V_{\rm SO}$ [Eq. (16) of Ref. 11] and subtract from them the pairwise sum of the gs pair potential interactions $V^{\rm gs}\{j\} = \sum_i V_{X^2\Sigma}(|\mathbf{r}_i^{\{j\}} - \mathbf{r}_{\rm Na}^{\{j\}}|)$ to obtain the excitation energy. The histogram of the collected stochastic energies is identified with the absorption spectrum, i.e.,

$$I(\omega) \propto \sum_m \frac{1}{n_c} \sum_{\{j\}}^{n_c} \delta\left[\omega - \left(V_m^{\rm ex}\{j\} - V^{\rm gs}\{j\}\right)/\hbar\right] . \quad (6)$$

In this way, we obtain the absorption spectrum of impurities in liquid helium including shape fluctuations. When this is the

main source of broadening, as for impurities embedded in the liquid or in the bulk of drops, the method has proved to reproduce fairly well the broadening of the absorption line, as we show for Mg in Sec. III. Note that other sources of broadening such as thermal wandering[20] or droplet size distribution effects may have a sizable influence for impurities residing in the outer surface of the droplet, and they are not accounted for by this procedure.

III. ABSORPTION SPECTRUM RESULTS

A. Na in mixed helium droplets

Figure 4 shows the absorption spectrum for Na@^{4}He$_{1000}$ +^{3} He$_{N_3}$ mixed droplets with $N_3 =$ 100,500,1000, and 3000. The vertical lines represent the location of the absorption lines of the free Na atom. As expected, the shift in the spectrum increases with the number of ^{3}He atoms.[3] In the ^{4}He$_{1000}$ +^{3} He$_{100}$ droplet, the effect of ^{3}He is barely perceptible and its spectrum is sensibly that of Na in the isotopically pure ^{4}He droplet. One might expect the impurity to draw the ^{3}He atoms and be quickly surrounded by them, but this is not quite so even for a more attractive impurity such as Ca.[24,28]

In the $N_3 = 1000$ and 3000 drops, it is the ^{4}He core that plays no significant role, and the spectrum is sensibly that of the isotopically pure ^{3}He droplet.[29] The $N_3 = 500$ droplet is an intermediate case, in which there is enough ^{3}He to influence the absorption spectrum but the number of ^{3}He atoms is still small, and the density in the ^{3}He shell does not reach that of the liquid at saturation; see, e.g., Ref. 8 and Fig. 1. In this configuration, the shift is slightly smaller than in a pure ^{3}He drop, although the difference is too small to be detectable. We recall that the experiments have been carried out for isotopically pure droplets of about 5000 atoms. The calculated peaks are narrower than in the experiment because Na resides at the outer surface of the droplet and thermal wandering and droplet-size distribution effects should contribute to the broadening in a non-negligible way.[11]

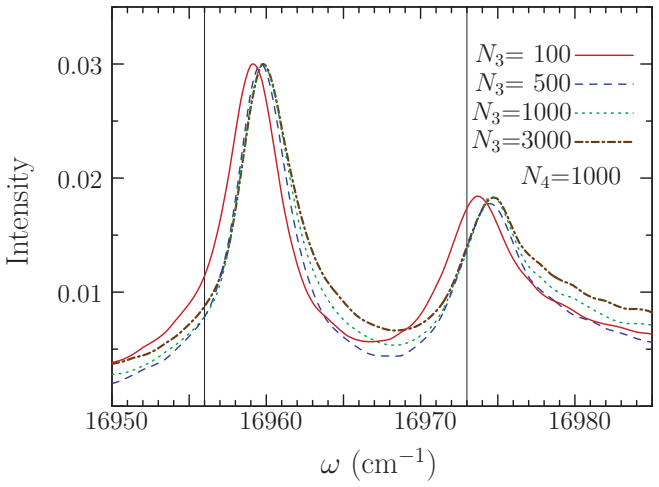

FIG. 4. (Color online) Absorption spectrum (arbitrary units) of Na in ^{4}He$_{1000}$+^{3}He$_{N_3}$ droplets with $N_3 = 100$ (solid line), 500 (dashed line), 1000 (dotted line), and 3000 (dash-dotted line). The thin vertical lines represent the gas-phase transitions. The spectra are normalized so that the more intense peaks all have the same height.

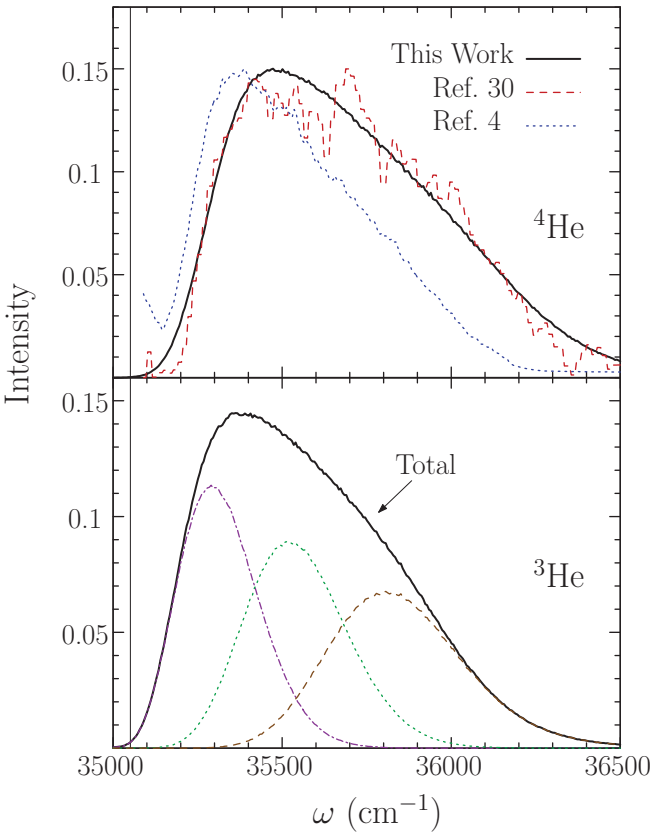

FIG. 5. (Color online) Top panel: Calculated absorption spectrum (arbitrary units) of Mg in liquid ^{4}He at $P = 0$ bar (solid line) compared to the experimental results of Refs. 30 (dashed line) and 5 (dotted line). The spectra are normalized so that the peaks have the same height. Bottom panel: Calculated absorption spectrum (arbitrary units) of Mg in liquid ^{3}He at $P = 0$ bar. The line has been decomposed into its two Π components and one Σ component, the latter one being the higher-energy transition. The thin vertical line represents the gas-phase transition.

B. Mg in liquid helium mixtures

Isotopic liquid helium mixtures are better suited than mixed drops to determine the effect of the isotopic composition on the absorption line, as one avoids finite-size effects and the actual composition of the fluid sample can be controlled. In addition, they offer the possibility to study the pressure effect on the spectrum.

The reason for choosing Mg atoms for this study is twofold. First, there are detailed results for its absorption spectrum in pressurized isotopically pure liquid ^{3}He and ^{4}He,[5,30] indicating that the shift in the absorption peak is about 100 cm^{-1} smaller in ^{3}He than in ^{4}He.[5] It is thus reasonable to expect that the absorption spectrum may show some sensitivity to the isotopic composition of the mixture. Secondly, the adiabatic Mg-He pair potentials for the ground[13] and excited states[19] are known with good accuracy. We want to mention the existence of a series of recent studies of Mg in helium droplets aimed at ascertaining whether this impurity resides in the

bulk or at the surface of ^{4}He drops.[19,20,31–33] Most studies point toward a sizable radial delocalization of Mg inside large drops.

In a first stage, we have computed the absorption spectrum of Mg in isotopically pure liquid ^{4}He and ^{3}He. For the former, there are two inconsistent sets of experimental data obtained by the same group, both of which are compared with our calculations in the top panel of Fig. 5. No detailed results for the line shape in the case of ^{3}He have been published for comparison. We remind the reader that our calculations are at $T = 0$, whereas the experiments have been carried out at 1.4 K.

While our calculations compare very well with the experimental results for ^{4}He in Ref. 30, they are blueshifted with respect to those of Ref. 5 for ^{4}He and ^{3}He as well. Despite this discrepancy, we have found, in agreement with the experimental findings,[5] that the shift is 0.77 nm larger in bulk ^{4}He than in bulk ^{3}He. This is an important check to assure that the calculation may disclose effects associated with the isotopic composition of the liquid mixture, as shown below.

The pressure dependence of the absorption spectrum of Mg in isotopically pure liquid ^{4}He and ^{3}He is shown in Fig. 6 for $P = 0$, 10, and 20 bar, and the peak energy is represented in Fig. 7 as a function of pressure. This dependence is in qualitative agreement with experiment,[5] although our results are systematically blueshifted with respect to the experimental results by about 1 nm. The crosses in Fig. 7 represent the peak energy slightly below the zero-temperature segregation line as a function of pressure. Thus, each point corresponds to a different x_3 value, as shown in Fig. 2. We conclude that the shift in the peak energy of the Mg absorption spectrum is significant. However, the size of the line can make it hard to determine experimentally the x_3 dependence. This is illustrated in Fig. 8, where we have drawn the absorption spectrum of Mg in an $x_3 = 9.4\%$ mixture at $P = 10$ bar. The absorption peak is shifted by 28 cm^{-1} with respect to the isotopically

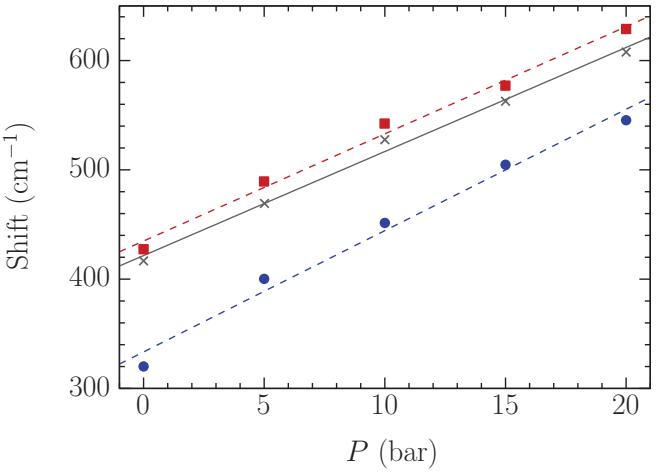

FIG. 7. (Color online) Peak energy shift of the absorption spectrum of Mg in isotopically pure liquid ^{4}He (squares) and ^{3}He (dots) as a function of pressure. The crosses represent the peak energy shift slightly below the segregation line for the corresponding pressures; the x_3 values are 6.3%, 8.9%, 9.4%, 9.2%, and 8.4% for $P = 0$, 5, 10, 15, and 20 bar, respectively. Least-squares linear fits for each set of points are drawn as a guide to the eye.

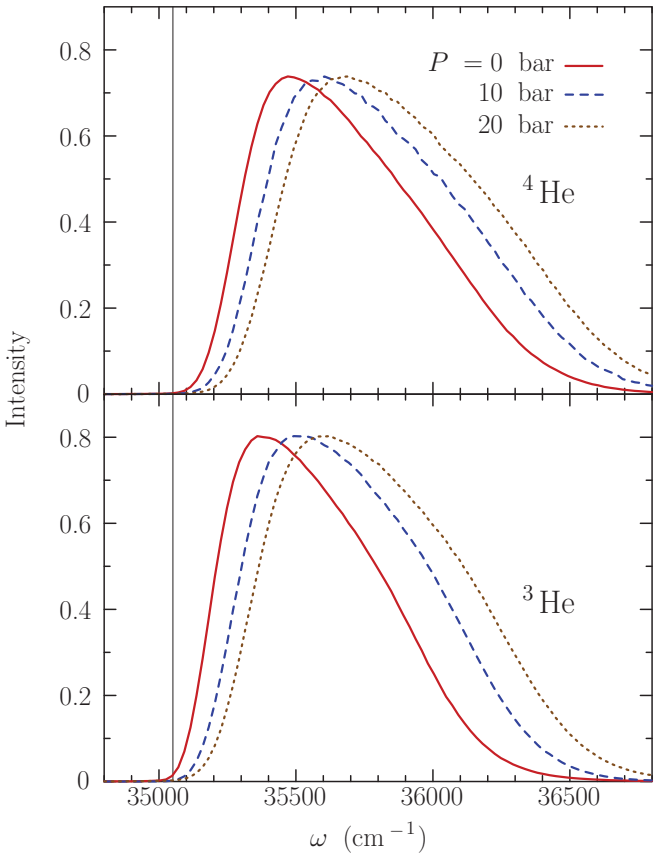

FIG. 6. (Color online) Top panel: Calculated absorption spectrum (arbitrary units) of Mg in liquid ^{4}He at $P = 0$ (solid line), 10 (dashed line), and 20 bars (dotted line). Bottom panel: Same as top panel for ^{3}He. The thin vertical line represents the gas-phase transition. The spectra are normalized so that the peaks have the same height.

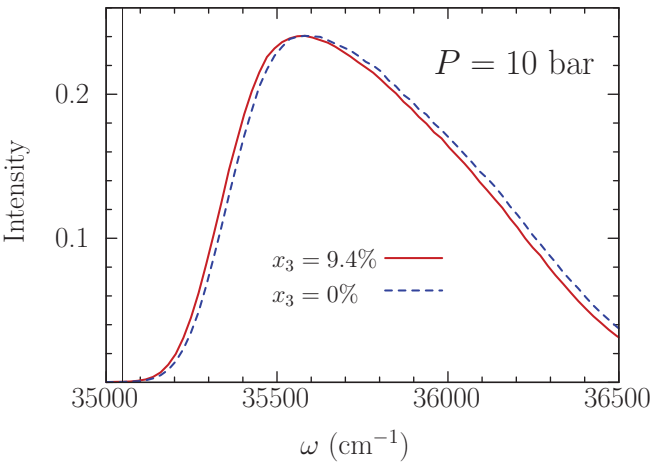

FIG. 8. (Color online) Absorption spectrum (arbitrary units) of Mg in an $x_3 = 9.4\%$ liquid mixture at $P = 10$ bar (solid line). The dashed line is the result for the isotopically pure liquid ^{4}He at the same pressure. The thin vertical line represents the gas-phase transition. The spectra are normalized so that the peaks have the same height.

pure liquid ^{4}He, in spite of the small morphological changes in the density profile introduced by this small ^{3}He amount (see Fig. 3).

IV. SUMMARY

We have studied the absorption spectrum of atomic impurities in mixed helium drops and liquid helium mixtures, paying special attention to the dependence of the spectrum on the ^{3}He concentration. For the study of drops, we have chosen Na as the impurity, which always resides on the surface of the drop, complementing the studies carried out in Ref. 6 for Ca.

For droplets of the size and composition addressed herein, we have found that the shift in mixed droplets is larger than in ^{4}He droplets but slightly smaller than in ^{3}He droplets. Even though a large amount of ^{3}He is needed for the density in the outer shell of the mixed droplet to reach the bulk liquid ^{3}He value, our results indicate that the spectrum of the impurity is very insensitive to the isotopic composition and it rapidly saturates to the value of pure ^{3}He droplets when the quantity of ^{3}He is increased. From this we infer that the effect of isotopic composition on the absorption spectrum is hardly detectable for alkali impurities in helium droplets. We have chosen Mg for the study of liquid mixtures, and we have compared the results obtained for isotopically pure liquid ^{4}He and ^{3}He with the experiments reported in Refs. 5 and 30. We have found that the peak energy in saturated helium mixtures can be shifted by up to some tens of cm^{-1} from that in pure ^{4}He at the same pressure. While much smaller atomic shifts from the gas-phase value have been detected experimentally, to determine the dependence of the atomic shift on the isotopic composition of the mixture is an experimental challenge due to the large width of the absorption line.

Finally, we would like to point out that the infrared spectrum of excess electrons might be a way to determine the structure of electron bubbles in isotopic mixtures of liquid helium, as it has been for isotopically pure liquid ^{4}He or ^{3}He.[34] Due to the electron-helium repulsion, electron bubbles are fairly large, with a radius of about 18.5 Å for ^{4}He and 22.5 Å for ^{3}He.[35] At variance with the situation for the small bubbles around an atomic impurity in liquid helium mixtures, the electron bubble surface should be coated by ^{3}He, as it is for bubbles appearing in homogeneous cavitation processes.[15] This coating increases the bubble radius with respect to that of isotopically pure ^{4}He, as it decreases the surface tension of the liquid. Since the electron spectrum is very sensitive to the bubble radius, determining it would probe the structure of the electron bubble in the mixture. Knowledge of this structure has potential implications for cavitation in liquid helium mixtures.[36,37] Work is in progress to obtain the electron absorption energies in liquid helium mixtures.

ACKNOWLEDGMENTS

We would like to thank Frank Stienkemeier and Oliver Bünermann for useful exchanges. This work has been performed under Grants No. FIS2008-00421/FIS from DGI, Spain (FEDER), and No. 2009SGR01289 from Generalitat de Catalunya. D.M. has been supported by the ME (Spain) FPU program, Grant No. AP2008-04343. A.H. has been supported by the MICINN (Spain) FPI program, Grant No. BES-2009-027139.

APPENDIX

Ignoring normalization, which is irrelevant for the present discussion, the probability distribution we have chosen for sampling N helium atoms is

$$P^N(\{\mathbf{r}_i\}) = \prod_{i=1}^{N} \frac{\rho(\mathbf{r}_i)}{N} \prod_{j<i}^{N} \Theta(r_{ij} - h), \tag{A1}$$

where Θ is the step function. The atomic density $\langle \sum_i \delta(r - r_i) \rangle$ corresponding to this probability distribution is

$$\left\langle \sum_{i=1}^{N} \delta(r - r_i) \right\rangle = \rho(r) \int \left(\prod_{j=1}^{N-1} dr_j \Theta(|\mathbf{r}_j - \mathbf{r}| - h) \right) P^{N-1}(\{\mathbf{r}_i\}) \neq \rho(r). \tag{A2}$$

Hence, due to the He-He correlations introduced in P^N, the density of the system is not equal—and cannot be—to the DF particle density $\rho(r)$, and one has to do something to recover $\rho(r)$ back from the sampling. To do so, we have introduced a density dependence on h such that the integral appearing in Eq. (A2) is a constant that could be absorbed in the normalization. This cannot be done exactly, but if one assumes that $\rho(r)$ varies smoothly, i.e., $\nabla\rho(\mathbf{r}) \ll \rho(\mathbf{r})/h$, then the result of the integral can be written as a power series of $h^3\bar{\rho}(\mathbf{r})$, where $\bar{\rho}(\mathbf{r})$ is the coarse-grained density. Then, to turn the integral into a constant, we just need to add a density dependence in h of the form $h \propto \bar{\rho}(\mathbf{r})^{-1/3}$. This is the reason why we have chosen the hard-sphere radius R as expressed in Eq. (5).

[1] B. Tabbert, H. Günther, and G. zu Putlitz, J. Low Temp. Phys. **109**, 653 (1997).

[2] J. P. Toennies and A. F. Vilesov, Angew. Chem. Ind. Ed. **43**, 2622 (2004); F. Stienkemeier and K. K. Lehmann, J. Phys. B **39**, R127 (2006); M. Barranco, R. Guardiola, S. Hernández, R. Mayol, Jesús Navarro, and M. Pi, J. Low Temp. Phys. **142**, 1 (2006); J. Tiggesbäumker and F. Stienkemeier, Phys. Chem. Chem. Phys. **9**, 4748 (2007); M. Y. Choi, G. E. Douberly, T. M. Falconer, W. K. Lewis, C. M. Lindsay, J. M. Merrit, P. L. Stiles, and R. E. Miller, Int. Rev. Phys. Chem. **25**, 15 (2006); K. Szalewicz, *ibid.* **27**, 273 (2008).

[3] F. Stienkemeier, O. Bünermann, R. Mayol, F. Ancilotto, M. Barranco, and M. Pi, Phys. Rev. B **70**, 214509 (2004).

[4] Y. Moriwaki and N. Morita, Eur. Phys. J. D **33**, 323 (2005).

[5]Y. Moriwaki, K. Inui, K. Kobayashi, F. Matsushima, and N. Morita, J. Mol. Struct. **786**, 112 (2006).
[6]O. Bünermann, M. Dvorak, F. Stienkemeier, A. Hernando, R. Mayol, M. Pi, M. Barranco, and F. Ancilotto, Phys. Rev. B **79**, 214511 (2009).
[7]S. Grebenev, J. P. Toennies, and A. F. Vilesov, Science **279**, 2083 (1998).
[8]M. Pi, R. Mayol, and M. Barranco, Phys. Rev. Lett. **82**, 3093 (1999).
[9]D. O. Edwards and M. S. Pettersen, J. Low Temp. Phys. **87**, 473 (1992).
[10]M. Barranco, M. Pi, S. M. Gatica, E. S. Hernández, and J. Navarro, Phys. Rev. B **56**, 8997 (1997).
[11]A. Hernando, M. Barranco, R. Mayol, M. Pi, and M. Krośnicki, Phys. Rev. B **77**, 024513 (2008).
[12]S. H. Patil, J. Chem. Phys. **94**, 8089 (1991).
[13]R. J. Hinde, J. Phys. B **36**, 3119 (2003).
[14]D. Mateo, M. Pi, and M. Barranco, Phys. Rev. B **81**, 174510 (2010).
[15]M. Guilleumas, D. M. Jezek, M. Pi, M. Barranco, and J. Navarro, Phys. Rev. B **51**, 1140 (1995).
[16]M. Lax, J. Chem. Phys. **20**, 1752 (1952).
[17]F. O. Ellison, J. Am. Chem. Soc. **85**, 3540 (1963).
[18]J. Pascale, Phys. Rev. A **28**, 632 (1983).
[19]M. Mella, G. Calderoni, and F. Cargnoni, J. Chem. Phys. **123**, 054328 (2005).
[20]A. Hernando, M. Barranco, R. Mayol, M. Pi, and F. Ancilotto, Phys. Rev. B **78**, 184515 (2008).
[21]H. J. Maris and W. Guo, J. Low Temp. Phys. **137**, 491 (2004).
[22]S. Ogata, J. Phys. Soc. Jpn. **68**, 2153 (1999).
[23]M. Mella, M. C. Colombo, and F. G. Morosi, J. Chem. Phys. **117**, 9695 (2002).
[24]R. Guardiola, J. Navarro, D. Mateo, and M. Barranco, J. Chem. Phys. **131**, 174110 (2009).
[25]T. Nakatsukasa, K. Yabana, and G. F. Bertsch, Phys. Rev. A **65**, 032512 (2002).
[26]A. Hernando, M. Barranco, R. Mayol, M. Pi, F. Ancilotto, O. Bünermann, and F. Stienkemeier, J. Low Temp. Phys. **158**, 105 (2010).
[27]A. Hernando, R. Mayol, M. Pi, M. Barranco, I. S. K. Kerkines, and A. Mavridis, Int. J. Quantum Chem. **111**, 400 (2011).
[28]D. Mateo, M. Barranco, R. Mayol, and M. Pi, Eur. Phys. J. D **52**, 63 (2009).
[29]Due to an unfortunate mistake in the calculation of the spectra, by which the mean gs potential interaction was used in Eq. (6) instead of its stochastic value, the calculated shift for ^{3}He droplets in Ref. 26 is in error.
[30]Y. Moriwaki and N. Morita, Eur. Phys. J. D **5**, 53 (1999).
[31]J. Reho, U. Merker, M. R. Radcliff, K. K. Lehmann, and G. Scoles, J. Chem. Phys. **112**, 8409 (2000).
[32]Y. Ren and V. V. Kresin, Phys. Rev. A **76**, 043204 (2007).
[33]A. Przystawik, S. Göde, T. Döppner, J. Tiggesbäumker, and K-H. Meiwes-Broer, Phys. Rev. A **78**, 021202(R) (2008).
[34]C. C. Grimes and G. Adams, Phys. Rev. B **45**, 2305 (1992).
[35]V. Grau, M. Barranco, R. Mayol, and M. Pi, Phys. Rev. B **73**, 064502 (2006).
[36]M. Barranco, M. Guilleumas, M. Pi, and D. M. Jezek, in *Microscopic Approaches to Quantum Liquids in Confined Geometries*, edited by E. Krotscheck and J. Navarro (World Scientific, Singapore, 2002).
[37]H. J. Maris, J. Phys. Soc. Jpn. **77**, 111008 (2008).